JOURNAL OF MATERIALS SCIENCE **34** (1999) 3299–3306

Kinetic studies on hot-stretching of polyacrylonitrile-based carbon fibers by using internal resistance heating

Part I *Changes in resistivity and strain*

H. S. KIM, M. SHIOYA*
Department of Organic and Polymeric Materials, Tokyo Institute of Technology, 2-12-1 O-okayama, Meguro-ku, Tokyo 152-8552, Japan
E-mail: mshioya@o.cc.titech.ac.jp

A. TAKAKU
Department of Life Culture, Seitoku University, 531 Sagamidai, Matsudo-shi, Chiba 271, Japan

The effects of the stretching stress applied during high temperature heat-treatment of polyacrylonitrile(PAN)-based carbon fibers on the structural development and the properties of the fibers were investigated kinetically using internal resistance heating. The temperature-time superposition could be applied to the changes in structural parameters, resistivity and tensile strength during heat-treatment using the same shift factors. The application of the stretching stress effectively reduced the fractions of slower rate processes and the activation energy of the structural development in the temperature region below about 1800 °C, and also influenced on the structural features. The longitudinal strain induced during heat-treatment increased in proportion to the logarithmic treatment time, showing different kinetics from that of the structural development.

1. Introduction

The conventional process to produce polyacrylonitrile(PAN)-based carbon fibers involves two different steps; a low temperature heat-treatment under oxidizing conditions for rendering the starting fibers infusible and a succeeding high temperature heat-treatment in inert atmosphere for developing oriented carbon structure. The tensile modulus of the resulting carbon fibers strongly depends on the preferred orientation of the crystallites since the crystallites in carbon fibers consist of carbon layer stacks having highly anisotropic properties [1]. The tensile modulus of carbon fibers tends to increase with increasing carbonization temperature owing to the development of oriented carbon structure. On the other hand, the tensile strength tends to be declined by heat-treatment at high temperatures [2, 3]. It has been shown, however, that if a stretching stress is applied to the fibers during heat-treatment, a higher tensile modulus is obtained without loss in tensile strength [4]. The effect of hot-stretching on the structure and mechanical properties of pitch- [5, 6] and PAN-based [7, 8] carbon fibers has been demonstrated. The kinetic studies of the structural development of carbon fibers under stretching stresses are required not only from the scientific view point but also for optimizing the temperature-time-stretching stress conditions. This study intends to elucidate the kinetics of structural development of PAN-based carbon fibers under stretching stresses.

The partially carbonized PAN fibers, which are obtained by carbonization at around 1000 °C, have increased electrical conductivity. Thus, it is possible to heat-treat the partially carbonized fibers at a higher temperature by use of the Joule heat generated by passing electric current through the fibers. This internal resistance heating is advantageous for the kinetic studies of the structural development of carbon fibers under stretching stresses for the following reasons: Firstly, the fibers can be heated to desired temperatures almost instantaneously [9, 10]. Thus, the influence of the heat-treatment which is inevitably made during the heating process of the isothermal experiments can be minimized. Secondly, the treatment time can be extended to a shorter region and the structural changes taking place over decades of time scale can be investigated in a reasonable time. Thirdly, the longitudinal strain of the fibers induced by the stretching stress can be accurately measured under rigorous temperature-time conditions since the elongation takes place over the well defined hot zone length. If the conventional furnace is used, the

* Author to whom all correspondence should be addressed.

temperature of the fibers usually distributes along the fiber length and the elongations taking place in different temperature regions contribute to the total change of the fiber length.

In this study, the internal resistance heating is used for the heat-treatments, under stretching stresses, of partially carbonized PAN fibers. The changes in resistivity and longitudinal strain of the fibers are measured during heat-treatments and the changes in the structural parameters and mechanical properties are measured on the heat-treated fibers. The experimental results are kinetically analyzed by assuming that the structural change can be represented by a superposition of first-order rate processes with a range of rate constants having an identical temperature dependence. This assumption has been verified with respect to the graphitization behavior of various graphitizing carbons [11–14] and the carbonization behavior of PAN- and pitch-based carbon fibers [15, 16]. In part I of the study, the changes in resistivity and longitudinal strain are reported. The changes in structural parameters and mechanical properties will be reported in detail in part II of the study [17].

2. Experimental

2.1. Fibers

The PAN-based carbon fibers processed at a maximum temperature of 1250 °C were used for the starting fibers of the internal resistance heating. These fibers were in the form of a tow comprising 3000 continuous filaments and the linear density of the tow was 0.202 gm^{-1}. The tensile modulus and the strength of the fibers were 255 and 3.92 GPa, respectively.

2.2. Internal resistance heating

A carbon fiber tow was extended horizontally in a Pyrex glass tube in contact with four graphite pulleys 2 cm in diameter as shown in Fig. 1. In order to bind closely the filaments in the tow, a twist of one turn per 5 cm was given to the tow. The external tensile load was applied to the tow by suspending dead weights from one end of the tow through a guide pulley. The length change of the tow was detected with a pulley and angular detector. Nitrogen gas was caused to flow in the glass tube at a rate of 5000 cm^3 min^{-1}. The electric current was passed through the tow using a pair of inner pulleys 10 cm apart as electrodes. The electric current was regulated so as to heat the tow according to a desired temperature-time profile. The surface temperature of the tow was measured by using an infrared radiation thermometer (Minolta IR-630), and the measured value will be quoted as the treatment temperature. The infrared transmittance of the glass tube at the wave lengths detected with the thermometer, 0.8–1.1 μm, was 0.81. The emissivity of the carbon fiber tow was assumed to be 0.9. These values were used to determine the surface temperature.

The heat-treatment was carried out as follows: First, a tow was heated at 600 °C for 30 min for conditioning. After the tow was cooled down to a room temperature, a dead weight of desired mass was suspended. Then, the tow was heated up to a desired temperature instantaneously and was kept at this temperature for a desired duration. Immediately after the heat-treatment was finished, the electric power was turned off and the tow was left cooling in the apparatus down to a room temperature within a few seconds.

2.3. Resistivity

The resistivity of the carbon fibers, ω, during heat-treatment was calculated using the equation,

$$\omega = ES(IL)^{-1} \quad (1)$$

where L is the distance between the electrodes; S is the cross-sectional area of the fibers; and E and I are the electric voltage and current applied to the tow. The

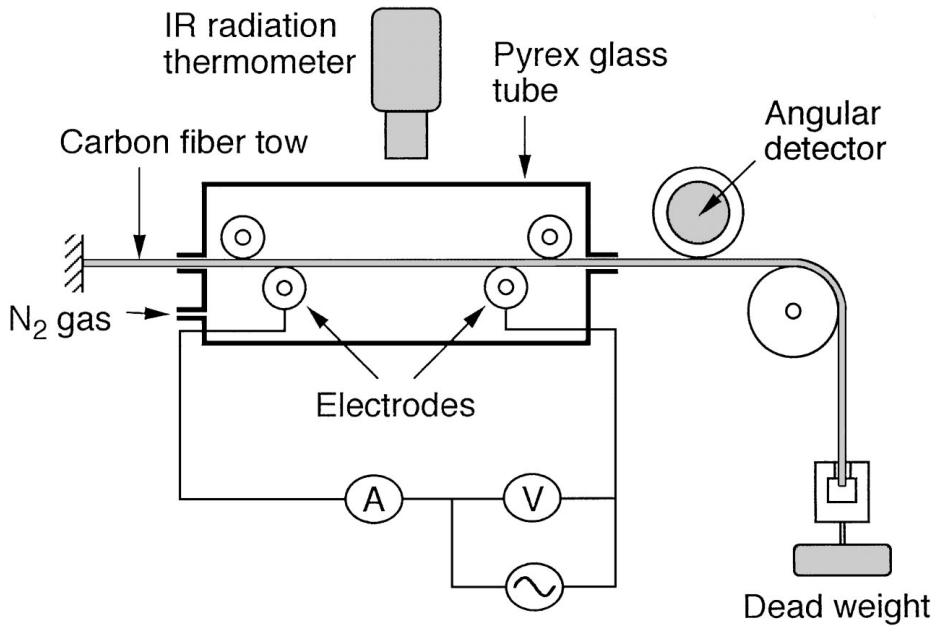

Figure 1 Schematic illustration of apparatus used for internal resistance heating of carbon fiber tow.

cross-sectional area of the fibers was estimated from the diameter of the heat-treated fibers measured at a room temperature.

2.4. Longitudinal strain

The fibers increased their length during heat-treatments under stretching stresses. By considering a fiber which is heat-treated uniformly over a whole fiber length all through the treatment, we shall define the longitudinal strain of the fiber, ε, as the ratio of the increase of the fiber length against the initial fiber length. For the present experimental apparatus, however, the distance between the electrodes was fixed. A part of the two moved out of the hot zone during the heat-treatment and this part of the tow was not heat-treated thereafter. Thus, the longitudinal strain, ε, was calculated from the measured length increase of the tow, ΔX, by the equation,

$$\varepsilon = \exp(\Delta X/L) - 1 \tag{2}$$

where L is the distance between electrodes.

The measurement of the length change was started after the dead weight was suspended and before the fibers were heated. Thus, the elastic deformations of the heating apparatus and the part of the tow outside of the hot zone were eliminated from the measured length change.

2.5. Fiber diameter

The diameter of the heat-treated fibers was measured using the diffraction of He-Ne laser beam by the single filament. The fiber diameter, D, was calculated using the equation,

$$D = \lambda(2\sin\theta)^{-1} \tag{3}$$

where λ is the wavelength of the laser beam and 2θ the scattering angle of the intensity minimum of the first order.

3. Analysis

In the usual thermally activated process, the rate constant, k, depends on temperature through an equation

$$k = A\exp(-\Delta H[RT]^{-1}) \tag{4}$$

where R is the gas constant; A is the frequency factor independent of temperature; ΔH is the activation energy; and T is the absolute temperature. Thus the rate constant at an arbitrary temperature, T, can be related to the rate constant, k_0, at the reference temperature, T_0, by the equation,

$$\begin{aligned} k &= \kappa(T)k_0 \\ &= \exp\left(-\Delta H[RT]^{-1} + \Delta H_0[RT_0]^{-1}\right)k_0 \end{aligned} \tag{5}$$

This equation represents the general case in which the activation energy values, ΔH and ΔH_0, at different temperatures T and T_0 are not necessarily equal. In the temperature region where the temperature dependence of ΔH is small, the activation energy can be obtained from the plots of $\ln\kappa(T)$ versus reciprocal temperature using the equation,

$$\Delta H = -R\,\mathrm{d}\ln\kappa(T)/\mathrm{d}T^{-1} \tag{6}$$

If the resistivity of carbon fibers, ω, changes with time, t, according to first-order rate processes with distributed rate constants, the resistivity changes as follows:

$$\begin{aligned} \omega &= \omega_\infty + (\omega_0 - \omega_\infty)\int_{-\infty}^{\infty} G(\ln k)\exp(-kt)\,\mathrm{d}\ln k \\ &= \omega_\infty + \int_{-\infty}^{\infty} F(\ln k)\exp(-kt)\,\mathrm{d}\ln k \end{aligned} \tag{7}$$

where ω_0 and ω_∞ are the initial and finally reached values of the resistivity; $G(\ln k)$ is the rate constant spectrum; and $F(\ln k)$ is the rate constant spectrum which involves the maximum resistivity change $(\omega_0 - \omega_\infty)$. In the following, $F(\ln k)$ will be simply called the rate constant spectrum. It is known that if the exponential function is approximated as

$$\exp(-kt) = \begin{cases} 1 - (kt/2) & (0 \le t \le 2/k) \\ 0 & (2/k \le t) \end{cases} \tag{8}$$

the rate constant spectrum can be obtained by using the equation

$$F(\ln k) = \left[\partial^2\omega/\partial(\ln t)^2\right] - \left[\partial\omega/\partial(\ln t)\right] \quad \text{where } t = 2/k \tag{9}$$

When the temperature is changed from T_0 to T, the rate constant changes from k_0 to k according to Equation 5. If, however, no rate process emerges nor disappears by the change of the temperature, the fractions of the rate processes are unchanged. That is,

$$F(\ln k)\,\mathrm{d}\ln k = F_0(\ln k_0)\,\mathrm{d}\ln k_0 \tag{10}$$

where F_0 $(\ln k_0)$ is the rate constant spectrum at the temperature T_0. Thus, Equation 7 can be modified as

$$\omega = \omega_\infty + \int_{-\infty}^{\infty} F_0(\ln k_0)\exp(-k_0 t_0)\,\mathrm{d}\ln k_0 \tag{11}$$

where

$$t_0 = \kappa(T)t \tag{12}$$

If the activation energy is constant for all the rate processes involved, $\kappa(T)$ takes a unique value for all the rate processes. Then, the resistivity change at the reference temperature given by Equation 11 can be obtained from the resistivity change at an arbitrary temperature given by Equation 7, by converting the treatment time t into the reduced time t_0 using Equation 12. This means that a composite curve of the resistivity change at the reference temperature over a wide range of time can be obtained by shifting the resistivity versus $\log_{10}t$ diagrams measured at various temperatures along the $\log_{10}t$ axis by the amount $\log_{10}\kappa(T)$.

With respect to the graphitizing behavior of various graphitizing carbons, the validity of the assumptions introduced in the treatments shown above has been verified [11–14]. It has been shown that these treatments can

be applied also to the carbonization behavior of PAN- and pitch-based carbon fibers [15, 16]. Thus, in this study, the effects of the stretching stress on the changes in the structure, resistivity and mechanical properties of PAN-based carbon fibers will be investigated by applying these treatments.

4. Results

4.1. Resistivity

Fig. 2 shows the resistivity change of the carbon fibers during isothermal heat-treatments under different stretching stresses. By superimposing these curves, smooth composite curves at a reference temperature of 1200 °C were successfully obtained as shown in Fig. 3. Thus, the temperature-time superposition is applicable to the resistivity change under stretching stresses.

The shift factors, $\log_{10}\kappa(T)$, used for temperature-time superposition are plotted against the reciprocal treatment temperature in Fig. 4. The temperature dependence of the shift factor differs between the temperature regions below and above 1800 °C, indicating that the activation energy differs between these temperature regions. The activation energies calculated in the temperature regions below and above 1800 °C were respectively 747 and 1166 kJ mol^{-1} at the stretching stress of 70 MPa, and 447 and 919 kJ mol^{-1} at the stretching stress of 322 MPa. Thus, the stretching stress effectively reduces the activation energy at temperatures below 1800 °C. The activation energy of the structural development of various graphitizing carbons is also appreciably higher at higher temperatures than at lower temperatures [14, 18].

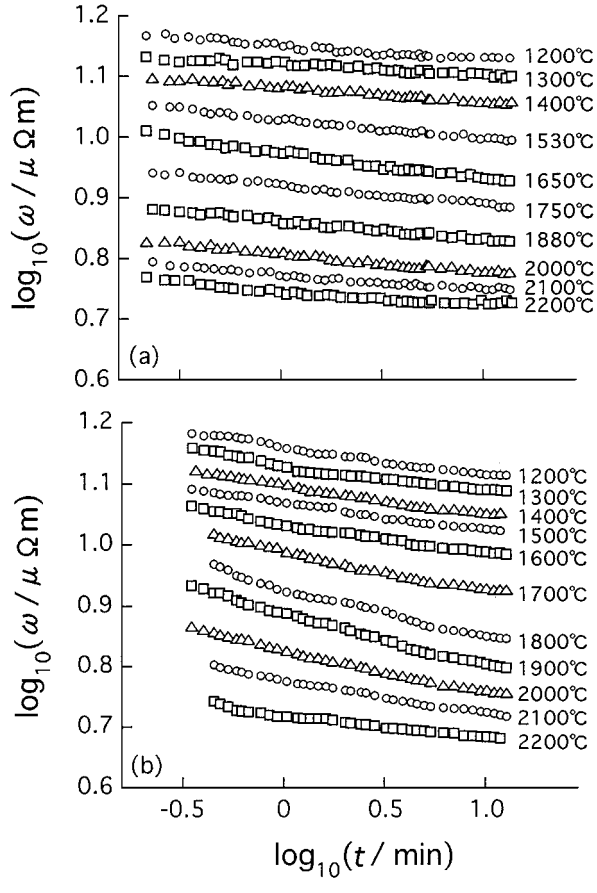

Figure 2 Resistivity, ω, versus treatment time, t, for isothermal heat-treatment of carbon fibers. Stretching stresses were (a) 70 and (b) 322 MPa and treatment temperatures are shown in the figure.

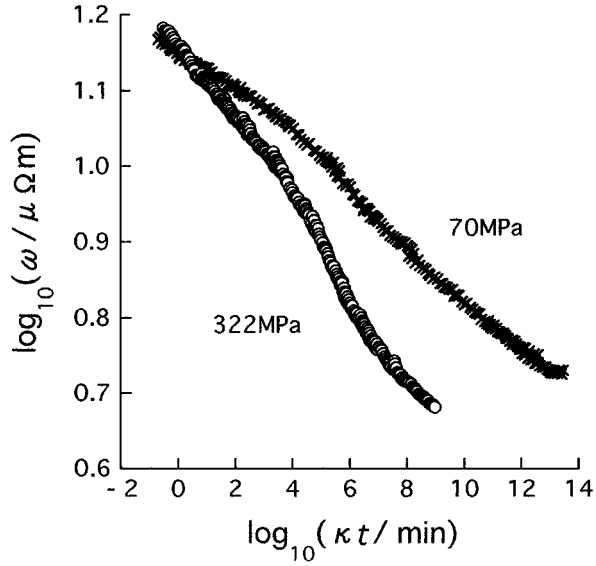

Figure 3 Composite curves of resistivity, ω, versus reduced time, $\kappa(T)t$, for isothermal heat-treatment of carbon fibers at 1200 °C. Stretching stresses are shown in the figure.

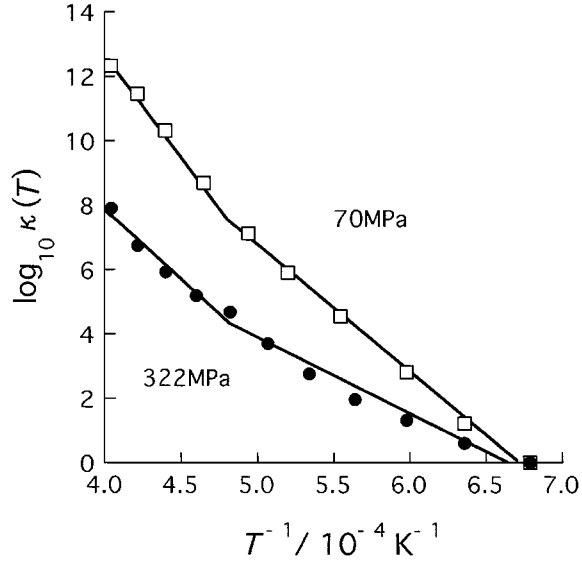

Figure 4 Shift factor, $\log_{10}\kappa(T)$, used for superimposing isothermal resistivity changes of carbon fibers referring to temperature of 1200 °C versus reciprocal treatment temperature, T. Stretching stresses are shown in the figure.

The rate constant spectra obtained from the composite curves of Fig. 3 are shown in Fig. 5 as a function of $\log_{10}(1/k)$, where $1/k$ stands for the treatment time at which values of $(\omega - \omega_\infty)$ for individual rate processes reduce to $(\omega_0 - \omega_\infty)/e$. Suppose that the treatment temperature is increased, rate constants are increased and the rate constant spectrum is shifted along ln k axis toward larger values by the amount determined by Equation 5. Suppose that a pretreatment is carried out on the specimen, a portion of the structural change is expended while the rate constants are unchanged. Thus, the rate constant spectrum is modified to $\exp(-k_0 t_0')F_0(\ln k_0)$, where t_0' is the reduced time of the pretreatment. Suppose that the activation energy is decreased, the rate

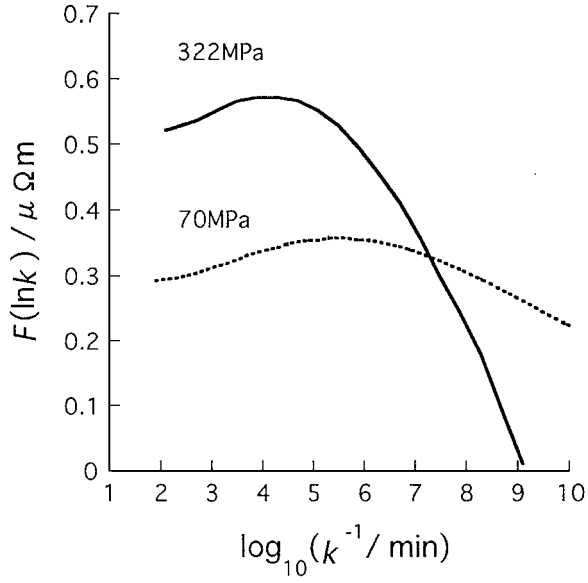

Figure 5 Rate constant spectra, $F(\ln k)$, as a function of logarithm of reciprocal rate constant, k, for carbon fibers at 1200 °C. Stretching stresses are shown in the figure.

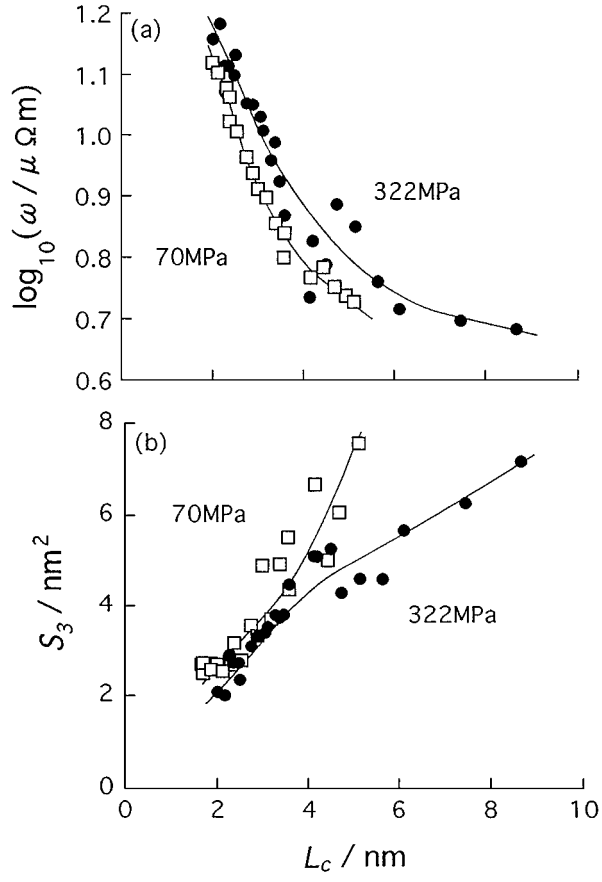

Figure 6 (a) Resistivity, ω, and (b) average area of microvoid cross-sections perpendicular to fiber axis, S_3, versus carbon layer stack height, L_c, for isothermally heat-treated carbon fibers. Stretching stresses are shown in the figure and various temperature-time conditions were used.

constants are increased and the rate constant spectrum is shifted along $\ln k$ axis toward larger values by the amount determined by the decrement of the activation energy. The observed influence of the stretching stress on the rate constant spectrum, however, is neither the shift of the spectrum along $\ln k$ axis nor the modification of the spectrum by the factor $\exp(-k_0 t_0')$. Thus, the effects of the stretching stress are different from those shown above and the similar effects can not be achieved merely by increasing the treatment temperature nor time. By applying a larger stretching stress, the fractions of slower rate processes are diminished while those of the faster rate processes are increased.

4.2. Structure and mechanical properties

The effects of stretching stress on the structural change and the mechanical properties of PAN-based carbon fibers will be reported in detail in the succeeding paper [17]. Several characteristic features, however, are briefly shown in the following in order to facilitate the discussions made in this paper.

In Fig. 6a, the resistivity of carbon fibers measured during isothermal heat-treatments are plotted against the carbon layer stack height, L_c, of the crystallites in the fibers. The carbon layer stack height was determined from the (002) wide-angle X-ray diffraction peak width of the fibers which were heat-treated using the same temperature-time-stretching stress conditions as the resistivity measurements. Under a constant stretching stress, the resistivity is uniquely related to the crystallite sizes, irrespective of the temperature-time conditions. This implies that the temperature-time superposition, using the shift factors determined from the resistivity change, is applicable to the change of the carbon layer stack height.

Some of the crystallite and microvoid parameters are uniquely related to the carbon layer stack height. One example is shown in Fig. 6b for the average area of microvoid cross-sections perpendicular to the fiber axis, S_3, which was determined from the equatorial small-angle X-ray scattering (SAXS) by using a method proposed by the present authors [19–21]. For the changes of these parameters, the temperature-time superposition, using the shift factors determined from the resistivity change, is also applicable.

Fig. 7 shows the composite curves at the reference temperature of 1200 °C thus obtained for the changes in crystallite orientation parameter, microvoid volume fraction, v_p, and tensile strength. In these figures, the crystallite orientation parameter was calculated from the full-width at half-maximum intensity (FWHM) of the azimuthal (002) diffraction intensity distribution as 1-(FWHM/π). The microvoid volume fraction was calculated from the equatorial SAXS [19–21]. The tensile strength was determined on single filaments. The smooth composite curves for the changes in interlayer spacing, carbon layer extent, carbon layer stack height, microvoid cross-section area and fiber density will be shown in the succeeding paper [17].

Since the application of a larger stretching stress reduces the fractions of slower rate processes, it is expected that the structural parameters change with a faster rate. This can be revealed in the change of the crystallite orientation parameter shown in Fig. 7a. Thus, the tensile modulus of the fibers increases at a faster rate when a larger stretching stress is applied during heat-treatment.

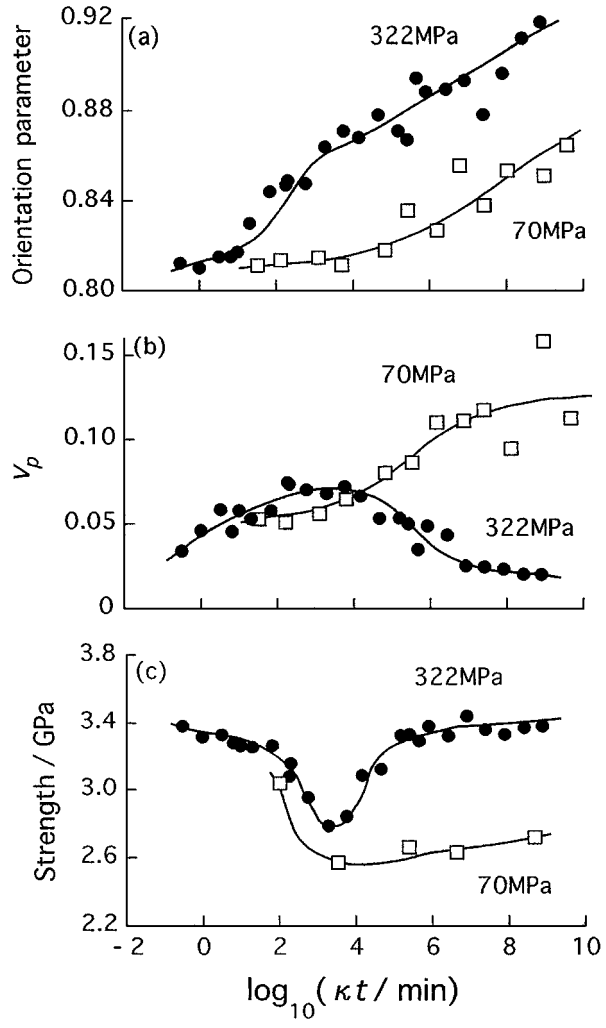

Figure 7 Composite curves of (a) crystallite orientation parameter, (b) microvoid volume fraction, v_p, and (c) tensile strength versus reduced time, $\kappa(T)t$, for carbon fibers isothermally heat-treated at 1200 °C. Stretching stresses are shown in the figure. Composite curves were constructed by using shift factors determined from resistivity change.

There are additional effects of stretching stress which cannot be achieved merely by increasing treatment temperature nor time. That is, by the application of a larger stretching stress, the microvoid volume fractions are decreased at longer treatment times as shown in Fig. 7b. Furthermore, the size of the microvoids is decreased when compared at an equivalent carbon layer stack height as shown in Fig. 6b. These effects work in favor of increasing tensile strength. As shown in Fig. 7c, the tensile strength initially decreases with increasing treatment time while it markedly increases at longer treatment times when a larger stretching stress is applied. It can be concluded, therefore, that the application of the stretching stress changes the structural features of the fibers as well as reducing the fractions of the slower rate processes and the activation energy of the structural development.

4.3. Deformation during heat-treatment

In Fig. 8, the diameter, D, of the fibers isothermally heat-treated using various temperature-time-stretching stress conditions are plotted against the strain, ε, induced during heat-treatment. If the deformation of the fiber took place on the bases of constant volume, the

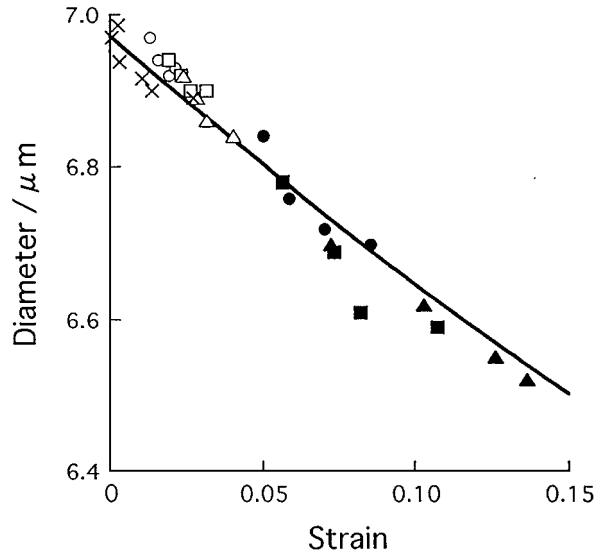

Figure 8 Fiber diameter versus longitudinal strain for isothermally heat-treated carbon fibers. Heat-treatments were carried out under stretching stress of 322 MPa at temperatures of (○) 1200, (□) 1400, (△) 1600, (●) 1800, (■) 2000 and (▲) 2200 °C for various durations, and (×) under stretching stress of 70 MPa using various temperature-time conditions.

value of $\pi D^2(1+\varepsilon)/4$ was kept constant. The solid line in Fig. 8 shows the best fit of this relationship to the experimental results. The fiber diameter changes almost following this relationship. Therefore, the reduction of the fiber diameter is brought about mainly by the plastic deformation rather than densification of the material accompanying release of the decomposed gases.

The longitudinal strain of the fibers induced by the isothermal heat-treatments under stretching stresses increases almost linearly with the logarithmic treatment time as shown in Fig. 9. This means that the strain rate is inversely proportional to the time in this time region. Similar time dependence has been observed for the creep strain of graphite [22, 23]. Jenkins [23] has shown that if the applied stress reduces the activation energy for the progress of plastic deformation and that the reduction of the activation energy decreases with increasing longitudinal strain according to its first order function, the strain increases in proportion to logarithmic time. The slope of the change in longitudinal strain with logarithmic time, $d\varepsilon/d\ln t$, is plotted against the temperature in Fig. 10. It is found that the strain rate increases remarkably by increasing the temperature above about 1800 °C, especially under a larger stretching stress.

It was tried to apply the temperature-time superposition, using the shift factors determined from the resistivity change, to the change of the longitudinal strain shown in Fig. 9 [17]. It was found that as the reduced time increased, the longitudinal strain at various temperatures increased at faster rates than what was expected from the temperature-time superposition, and the smooth composite curves could not be obtained.

5. Discussion

Fischbach [11, 14] has described the kinetics of graphitization as follows: Graphitization results from progressive removal of defects within and between carbon

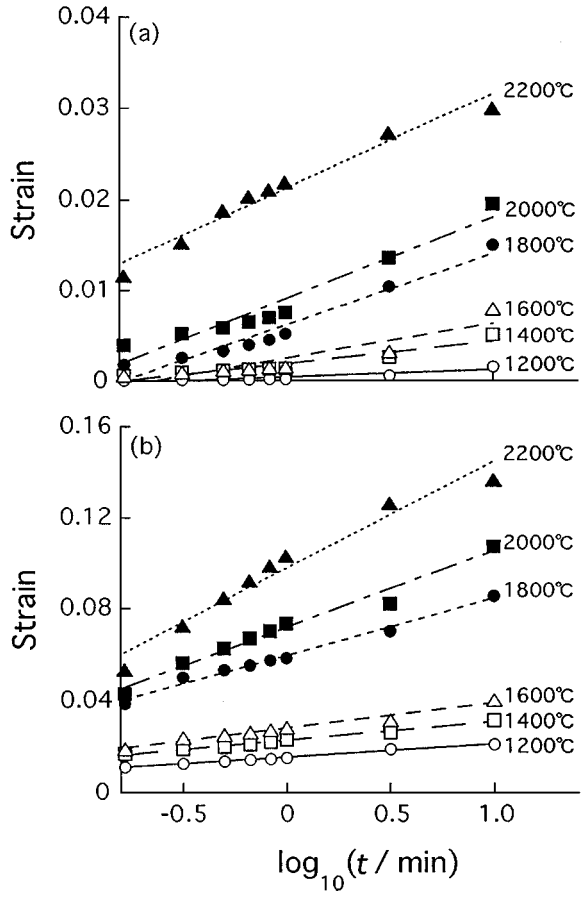

Figure 9 Longitudinal strain versus treatment time, t, for isothermal heat-treatment of carbon fibers. Stretching stresses were (a) 70 and (b) 322 MPa and treatment temperatures are shown in the figure.

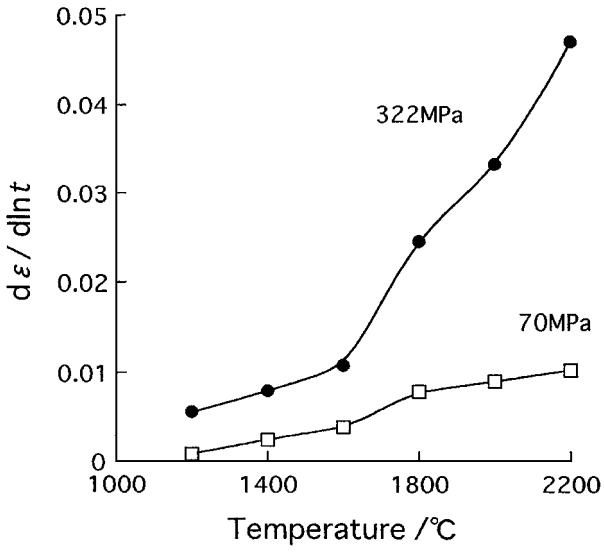

Figure 10 Slope of change of longitudinal strain with logarithmic treatment time, $d\varepsilon/d\ln t$, versus treatment temperature for isothermal heat-treatment of carbon fibers. Stretching stresses are shown in the figure.

layers, rather than the rearrangement of whole, perfect layers. There is a rate-determining, fundamental thermally activated process in graphitization, and this process can be attributed to the mass-transport self-diffusion by a defect mechanism. Thus, a single value of the activation energy of about 1000 kJ mol^{-1} is observed for a number of graphitizing carbons above about 2000 °C. Progress of graphitization is represented by a superposition of first-order rate processes with a range of frequency factors having a single value of the activation energy. This provides the bases for the temperature-time superposition. The distribution of the frequency factor results from differences in the amount of diffusion required to produce a detectable change in structure.

If the carbonization mechanism of the non-graphitizing carbons like PAN-based carbon fibers can be described similarly, the observed effects of stretching stress on the rate constant spectrum can be interpreted in terms of the reduction of the amount of diffusion required for the development of more perfect and flat carbon layers and their stacks. It seems likely that breaking of cross-link and dewrinkling of the carbon layers caused by stretching stress reduce the required amount of diffusion. Since the structure resulting from the mass-transport self-diffusion is the flat carbon layers extended in the fiber axis direction, it is possible that the strain energy produced by the stretching stress works in favor of reducing the activation energy.

The structural development accompanies the increase in the longitudinal strain of the fibers and this strain will be called the structure-dependent component of strain. The application of the stretching stress causes the change of the structural features of the resulting carbon fibers as is seen in the reduction of volume fractions and the relative sizes of microvoids. Thus, the application of the stretching stress changes the structure-dependent component of strain. This structure-dependent component of strain follows the same kinetics as that of the structural development. The measured longitudinal strain, however, changes with different kinetics, indicating that the longitudinal strain involves another component which is structure-independent. Slip between structural units such as microfibrils can be the source of the structure-independent component of strain. It is considered that at temperatures above about 1800 °C, slip between structural units is facilitated and the applied strain energy is not stored as the strain energy of the disordered structural units but dissipated through slip between structural units. Thus, the stretching stress at higher temperatures does not make significant contribution to the reduction of the energy which should be supplied for surmounting the energy barrier of the structural development. In contrast to the carbon fibers, graphite which has quite different structure from that of carbon fibers shows similar activation energy values both for the structure development and the creep behavior [14]. Thus, the structure-independent component of strain strongly depends on the structural features of carbons.

The experimental results showed that the activation energy at higher temperatures was higher irrespective of the stretching stress. This temperature dependence of the activation energy can not be attributed to the difference in the perfectness nor the sizes of the structure yielded at different temperatures. This is because if the perfectness or the sizes of the structure influences the activation energy, it results that the activation energy should also change with treatment time and that the

temperature-time superposition can not be applied. It has been suggested by a number of researchers that internal stress generated during heat-treatment makes an important contribution to the growth of the crystallites [14]. Therefore, it is considered that the internal stress is dissipated through the plastic deformation taking place at higher temperatures, leading to the increase in the energy which should be supplied for surmounting the energy barrier of the structural development.

6. Summary

The expression of the carbonization behavior in terms of a superposition of first-order rate processes with distributed frequency factors having a constant activation energy was also applicable to the structure change during heat-treatment of PAN-based carbon fibers under stretching stresses. The temperature-time superposition could be applied to the changes in the structure and resistivity, and apparently to the change in the tensile strength, using the same shift factors. The application of the stretching stress effectively reduced the fractions of slower rate processes and the activation energy of the structural development in the temperature region below about 1800 °C. The application of the stretching stress also caused change of the structural features of the fibers. The application of the stretching stress had effects which could not be achieved merely by increasing treatment temperature nor time. The longitudinal strain induced during isothermal heat-treatment increased almost in proportion to the logarithmic time and the strain rate increased markedly by the increase of the temperature above about 1800 °C. The longitudinal strain involved a component having different kinetics from that of the structural development. This component reduced the strain energy stored in the structural units, and diminished the contribution of the stretching and internal stresses to reduce the activation energy of the structural development.

References

1. W. RULAND, *Appl. Polym. Symp*. **9** (1969) 293.
2. R. MORETON, W. WATT and W. JOHNSON, *Nature* **213** (1967) 690.
3. J. W. JOHNSON, *Appl. Polym. Symp*. **9** (1969) 229.
4. J. W. JOHNSON, J. R. MARJORAM and P. G. ROSE, *Nature* **221** (1969) 357.
5. H. M. HAWTHORNE, *J. Mater. Sci*. **11** (1976) 97.
6. *Idem.*, in Proceeding of the International Conference on Carbon Fibers and their Composites (Plastics Institute, London, 1971), p. 81.
7. D. H. ISAAC, S. OZBEK and J. G. FRANCIS, *Mater. Manuf. Process*. **9** (1994) 179.
8. S. OZBEK and D. H. ISAAC, *ibid.* **9** (1994) 199.
9. K. YAMAMOTO, T. KIKUTANI and A. TAKAKU, *Tanso* **146** (1991) 8.
10. *Idem.*, *ibid.* **148** (1991) 142.
11. D. B. FISCHBACH, *Nature* **200** (1963) 1281.
12. T. NODA, M. INAGAKI and T. SEKIYA, *Carbon* **3** (1965) 175.
13. M. INAGAKI, Y. MURASE and T. NODA, *J. Ceram. Assoc. Japan* **76** (1968) 184.
14. D. B. FISCHBACH, in "Chemistry and Physics of Carbon," Vol. 7, edited by P. L. Walker, Jr. (Dekker, New York, 1968), pp. 1–105.
15. A. TAKAKU, T. MANGANZI and M. SHIOYA, *Tanso* **163** (1994) 119.
16. *Idem.*, *Carbon* **34** (1996) 1449.
17. H. S. KIM, M. SHIOYA and A. TAKAKU, *J. Mater. Sci.*, in press.
18. M. SHIRAISHI, in "Tanso Zairyou Nyuumon," edited by M. Inagaki (The Carbon Society of Japan, Tokyo, 1984), pp. 38–39.
19. M. SHIOYA and A. TAKAKU, *J. Appl. Phys*. **58** (1985) 4074.
20. *Idem.*, *J. Mater. Sci*. **21** (1986) 4443.
21. *Idem.*, *ibid*. **25** (1990) 4873.
22. H. W. DAVIDSON and H. H. W. LOSTY, *Nature* **4615** (1958) 1057.
23. G. M. JENKINS, *Phil. Mag.* **8** (1963) 903.

Received 30 June 1997
and accepted 28 January 1999